J. Phycol. **41,** 335–342 (2005)

DOI: 10.1111/j.1529-8817.2005.04034.x

CORAL PHOTOBIOLOGY STUDIED WITH A NEW IMAGING PULSE AMPLITUDE MODULATED FLUOROMETER[1]

Peter J. Ralph[2]

Institute for Water and Environmental Resource Management, and Department of Environmental Sciences, University of Technology, Sydney, Westbourne St. Gore Hill, NSW 2065 Australia

Ulrich Schreiber

Julius-von-Sachs Institut für Biowissenschaften, Universität Würzburg, Germany

Rolf Gademann

Gademann Meßtechnik, Dürrrbachtal, Würzburg, Germany

Michael Kühl

Marine Biological Laboratory, Institute of Biology, University of Copenhagen, Strandpromenaden 5, DK-3000 Helsingør, Denmark

and

Anthony W. D. Larkum

School of Biological Sciences, University of Sydney, NSW 2006, Australia

A new high-resolution imaging fluorometer (Imaging-PAM) was used to identify heterogeneity of photosynthetic activity across the surface of corals. Three species were examined: *Acropora nobilis* Dana (branching), *Goniastrea australiensis* Edwards & Haime (massive), and *Pavona decussata* Dana (plate). Images of fluorescence parameters (F, F_m', effective quantum yield, optimal quantum yield, electron transport rate, relative photosynthetic rate, and non-photochemical quenching) allowed heterogeneity to be detected in terms of position on colony and indicated that the photosynthetic activity of polyp and coenosarc tissues responded differently to changing light for all three species. The Imaging-PAM offers a special routine, with which images of PAR absorption (absorptivity) are obtained. In this way, for the first time it has become possible to derive images of the relative photosynthesis rate. Polyps had a lower PAR absorptivity than coenosarc tissue for *A. nobilis* and *P. decussata*, whereas *G. australiensis* showed the opposite pattern. *Acropora nobilis* showed heterogeneity along the longitudinal axis of the branch, which could be differentiated from the effect of variations in illumination across the rugose and curved surface. Diel changes were apparent and influenced the longitudinal heterogeneity along the *A. nobilis* branch. Images were also obtained showing the degree of photoinhibition caused by high-light stress across a coral surface at a hitherto unobtainable level of resolution.

Key index words: **corals; fluorescence; heterogeneity; Imaging-PAM; photosynthesis**

Abbreviations: **CCD, charge coupled device; E_k, minimum saturating irradiance; ETR, electron transport rate; LED, light-emitting diode; NIR, near infrared; NPQ, non-photochemical quenching; PAM, pulse amplitude modulated; PS, photosynthetic rate; RLC, rapid light curve**

Unicellular dinoflagellates (zooxanthellae) in corals provide photosynthetic products that are essential to the cnidarian host, and symbiont photosynthesis is therefore critical to the survival of corals. Coral reefs are characterized by rapid gradients in light, from shallow to deep water, from lit to shaded surfaces, and from light-exposed to highly light-filtered sites. Individual corals respond to changes in light in a wide diversity of ways. Heterogeneity of photosynthesis is a common observation in corals and other reef-dwelling organisms (Kühl et al. 1995, Ralph et al. 2002, Hill et al. 2004), varying across scales from millimeters (Kühl et al. 1995) up to the entire colony (Helmuth et al. 1997), with even greater variation occurring between colonies. Sun and shade adaptation of coral photosynthesis is an important phenomenon to which both zooxanthellae and the coral host contribute. This can be based on coral growth form and orientation (Jokiel and Morrissey 1986), such that sun-exposed tips are generally lighter in color (fewer zooxanthellae, and therefore lower in chl, per unit area) compared with lower branches, which contain a greater density of photosynthetic pigments (Falkowski et al. 1984). Many factors influence the distribution, density, and

[1]Received 19 March 2004. Accepted 22 June 2004.
[2]Author for correspondence: e-mail peter.ralph@uts.edu.au.

photosynthetic efficiency of corals (Gladfelter et al. 1989, Helmuth et al. 1997, Jokiel et al. 1997), including the presence of different genetic strains of zooxanthellae that may exhibit different photosynthetic capacity (Rowan and Knowlton 1995). At the scale of a single branch, microhabitat variations in light, water flow, and gas exchange appear to strongly influence the photosynthetic responses of *in hospite* zooxanthellae (Kühl et al. 1995, de Beer et al. 2000).

Heterogeneity occurs at the scale of millimeters where polyp and coenosarc tissue can exhibit different photosynthetic capacities (Kühl et al. 1995, Ralph et al. 2002). Zooxanthellae in the coenosarc tissue that connects polyps are more exposed to light than the more shade-adapted zooxanthellae within the polyp, which are located mostly within the endodermal layer inside the gastrodermal cavity. It has been suggested that the spacing of coral polyps can minimize self-shading and increase the efficiency of light capture (Jokiel and Morrissey 1986). Significant differences in oxygen production rates between polyp and coenosarc tissue of *Favia* sp. have been demonstrated, with highest rates in the polyp tissue (Kühl et al. 1995).

To map the spatial heterogeneity of photosynthesis, different chl fluorescence imaging systems have been developed (Omasa et al. 1987, Daley et al. 1989, Nedbal et al. 2000). The measuring principles applied range from relatively simple light modulation approaches (Siebke and Weis 1995a, Oxborough and Baker 1997, Grunwald and Kühl 2004) to advanced lifetime imaging systems (Holub et al. 2000). So far, most applications have involved terrestrial plants (Siebke and Weis 1995b, Chaerle and van der Straeten 2001), but the application of dynamic fluorescence imaging in aquatic systems is increasing rapidly (Oxborough et al. 2000, Berman-Frank et al. 2001, Hill et al. 2004, Grunwald and Kühl 2004).

A recently developed Imaging-PAM chl fluorometer (Schreiber et al. 2003) applies pulse amplitude modulated (PAM) measuring light (using blue light-emitting diodes [LEDs]) to map the chl *a* fluorescence yield with a spatial resolution of < 0.5 mm.The Imaging-PAM is fundamentally a two-dimensional version of the more common PAM chl fluorometers (Mini-PAM or Diving-PAM) that are widely used in coral research. It can perform all standard routines of saturation pulse quenching analysis (Schreiber 2004), such as determination of F_v/F_m and $\Delta F/F_m'$ (optimal and effective PSII quantum yield, respectively), as well as measurements of fluorescence induction and rapid light curves (RLCs) (Ralph et al. 2002). In addition, the Imaging-PAM offers a special routine in which images of PAR absorptivity are obtained. In this way, for the first time it has become possible to take heterogeneity in PAR absorption into account when deriving images of relative photosynthesis rate from dynamic fluorescence images.

In this study, we present the first assessment of spatial heterogeneity of coral tissues using a standard Imaging-PAM as well as a first prototype of a submersible Imaging-PAM. We used these instruments to map photosynthetic parameters across a variety of individual corals and under a range of light conditions. We demonstrate the utility of this device and illustrate several applications with corals, such as assessing photoinhibition and diel fluctuations in photosynthesis.

MATERIALS AND METHODS

Coral specimens. Shallow water colonies of three species of coral were used. *Acropora nobilis* (Dana) and *Goniastrea australiensis* (Edwards & Haime) were collected from the lagoon off Heron Island (152°06′ E, 20°29′ S), whereas *Pavona decussata* (Dana) was collected from the lagoon off One Tree Island (152°06′ E, 20°30′ S) between 26 January and 4 February 2003. Four replicate colonies of *G. australiensis* and *P. decussata* were collected from sun-adapted positions, whereas four sun-and four shade-adapted branches of *A. nobilis* were also collected. Both *A. nobilis* and *P. decussata* have thin tissues covering the skeleton, whereas *G. australiensis* has a thicker fleshy tissue. Corals were maintained before the experiment in aquaria flushed with natural seawater at 27° C under semi-shaded conditions (< 200 μmol photons $\cdot m^{-2} \cdot s^{-1}$) for 1 day.

Imaging-PAM chl a fluorometer. An Imaging-PAM chl fluorometer (Walz GmbH, Effeltrich, Germany) was used to investigate the spatial heterogeneity in photosynthetic parameters of three species of coral. The Imaging-PAM was composed of a high-speed charge coupled device (CCD) camera, an LED array, and a control unit to synchronize light emission by the LED array with the shutter opening of the camera (Fig. 1). The CCD camera had a resolution of 640 × 480 (307,200) pixels. Using a 12-mm lens (F1.2 with a focal distance of 70 mm), it was able to image an area of approximately 24 × 32 mm at a spatial resolution of 50 μm. The CCD was protected from stray excitation light by a long-pass filter (Schott, RG 645, Schott Standard Lighting, Southbridge MA, USA) and from long wavelength ambient light by a short-pass filter (Balzers, Hudson, NH, USA, Calflex-X, $\lambda < 780$ nm).

Images of fluorescence emission were digitized within the camera and transferred via a Firewire interface (400 megabits/s) (Firewire-1394, Austin, TX, USA) to a personal computer for storage and analysis. Measuring light pulses were applied at low frequency (about 1 Hz) for measurement of F_o images in quasi-dark state. During actinic illumination and saturation pulses, the frequency of measuring light pulses and image capture was automatically increased to about 10 Hz. Associated with each data acquisition step two images were measured, one shortly before the light pulse and one during the light pulse. The two images were subtracted from each other pixel by pixel, resulting in an image that was corrected for the ambient background light. The imaging system can thus tolerate background light by increasing the intensity of the measuring light and decreasing the gain of the CCD camera. With optimized settings, ambient daylight is tolerated.

The LED array contained 112 LEDs (mounted at a fixed angle for homogeneous illumination), two outer rings of blue LEDs (470 nm, 96 units), and within the inner ring 8 pairs of red (650 nm) and near-infrared (NIR, 770 nm) LEDs. The blue LEDs provided measuring light as well as actinic light and saturating light pulses, whereas the red and NIR LEDs were used for determination of PAR absorption (absorptivity). The absorptivity parameter is defined for every pixel as 1 − [R/NIR], where R is the pixel value of reflected light from pulse-modulated illumination by the red LEDs and NIR is the pixel value of reflected light from pulse-modulated illumination by the NIR LEDs. Although the R image is strongly affected by

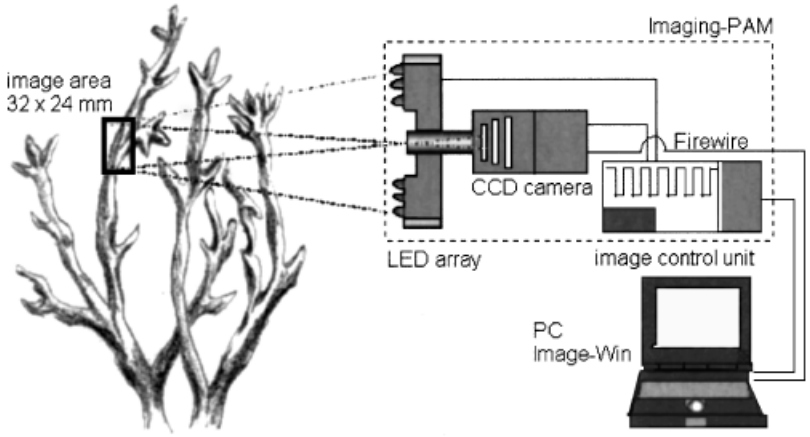

FIG. 1. Experimental setup and a schematic diagram of the Imaging-PAM system used for coral measurements. The Imaging-PAM consists of a CCD camera, an LED array, and a personal computer–controlled unit that synchronizes the LED emission and image capture.

the presence of photosynthetically active pigments, this is not the case for the NIR image. The system was calibrated by adjusting the R and NIR beams to give identical pixel values with a white piece of paper (PAR absorptivity, zero). In a healthy coral, where the red light was strongly absorbed by chl, the NIR signal could be 5-fold higher than red, so absorptivity is 0.80, meaning 80% absorption of the red light.

The Imaging-PAM continuously measured the current fluorescence yield (F_t). In the absence of actinic illumination, upon application of a saturating pulse the dark-level fluorescence yield (F_o) and the maximum fluorescence yield (F_m) were determined, from which the optimal PSII quantum yield (F_v/F_m) was calculated. In the presence of actinic illumination, the current fluorescence yield ($F_t = F$) and the maximum light-adapted fluorescence (F_m') were determined, from which the effective PSII quantum yield ($\Phi_{PSII} = [F_m' - F]/F_m' = \Delta F/F_m'$), electron transport rate ($ETR = \Phi_{PSII} \times PAR \times 0.5 \times 0.84$), and the relative photosynthetic rate ($PS = \Phi_{PSII} \times PAR \times 0.5 \times$ absorptivity) could be calculated. The Imaging-PAM distinguishes between ETR and PS, where the former assumes a homogenous absorption coefficient and the latter is based on a measured absorptivity image. PAR denotes the incident photosynthetically active radiation, the factor 0.5 corrects for an assumed equal distribution of the absorbed quanta between PSII and PSI, and 0.84 is a widely accepted absorptivity value for terrestrial leaves (Björkman and Demmig 1987). For image presentation, the apparent rate of photosynthetic electron transport was divided by 50 (PS/50) to maintain the pixel values within a normalized range (0–1).

Rapid light curve measurements (Schreiber et al. 1997) were obtained through the application of a series of 10-s light exposures with increasing irradiance (31, 81, 120, 185, 295, 385, 480, 610, and 770 μmol photons $\cdot m^{-2} \cdot s^{-1}$). Nonphotochemical quenching ($NPQ = [F_m - F_m']/F_m'$) was determined as the highest NPQ value on the RLC. Measured RLCs were fitted to a double exponential decay function:

$$P = P_s(1 - e^{-(\alpha\alpha_d/P_s)})e^{-(\beta\beta_d/P_s)} \quad (1)$$

Three parameters were derived from the fitted curves: the light-limited PS (α), the maximal photosynthesis at saturation (P_m), and the irradiance at onset of saturation ($E_k = P_m/\alpha$). For details on the curve-fitting routine used for RLC data, see Platt et al. (1980) or Hill et al. (2004).

A prototype of a submersible Imaging-PAM (Walz GmbH) was also used to measure the *in situ* changes in photosynthesis of corals during diel experiments. The submersible Imaging-PAM was functionally identical to the above-described standard unit, except for being encased in a waterproof cylinder (13 × 34 cm) with a glass window. For imaging at a fixed focal distance, a small bracket was mounted on the outside of the housing to outline the focal plane and area monitored by the submersible unit.

Experimental protocol. A series of RLC measurements were performed on samples of *A. nobilis*, *G. australiensis*, and *P. decussata* to demonstrate the corals' capacity to tolerate a range of different light intensities. For the photoinhibition experiment, samples of *A. nobilis* and *P. decussata* had a sheet of aluminum foil placed over most of the coral, leaving a small 2-mm slit uncovered (shown by the line running from the lower left corner of Ft images of both series; see Fig. 5). The corals were placed in semi-exposed flow-through aquaria for 20 min to induce a photoinhibitory response in the tissue exposed to ambient full sunlight at 10:00 a.m. (approximately 1000 μmol photons $\cdot m^{-2} \cdot s^{-1}$). Water movement was allowed under the foil to prevent development of anaerobic conditions due to impairment of gas exchange. Samples were dark-adapted for 5 min after the high-light treatment, before further experiments.

To demonstrate heterogeneity in diel variations in photosynthesis, a small colony of *A. nobilis* was placed in an outdoor flow-through aquarium. The submersible Imaging-PAM was used to capture data at intervals from 6:00 a.m. to 8:00 p.m. on 26 January 2003. The incident PAR irradiance during the experiment was measured with a quantum irradiance meter (LI-1400, Li-Cor, Lincoln, NE, USA).

Statistical analysis. Variation in the α, ETR_{max}, and E_k measurements for the polyp, coenosarc, tip, and base of branch were tested using a one-way analysis of variance model, where significance was tested at the 0.05 level. Assumptions of normality and equal variance were satisfied, thus allowing for the use of a parametric analysis. These analyses were performed using the software Systat, Chicago, IL, USA (version 8.0). To determine whether significant differences existed between the various regions, Tukey's pairwise test was applied (Sokal and Rohlf 1995).

RESULTS

The three species of coral showed remarkable variation in photosynthetic characteristics as well as topographic variation, linked to the structure of the individual coral sample (Fig. 2). Interestingly, the

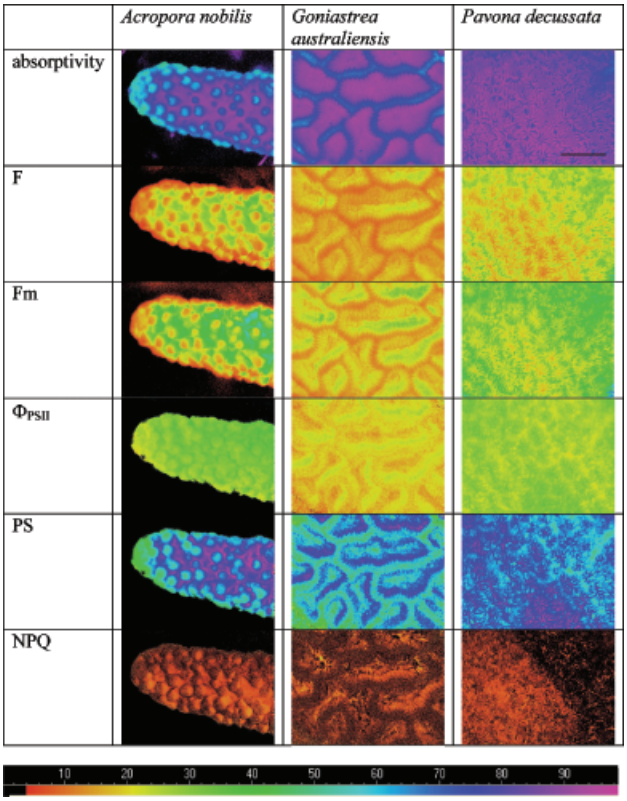

FIG. 2. Chl *a* fluorescence images of three corals species (*Acropora nobilis* [shade-adapted], *Goniastrea australiensis*, and *Pavona decussata*) showing PAR absorptivity, F, Fm′, the effective quantum yield (Φ_{PSII}), the relative photosynthesis rate (PS), and the nonphotochemical quenching coefficient (NPQ). All corals were exposed to an irradiance of 295 µmol photons $\cdot m^{-2} \cdot s^{-1}$. Relative values ranging from 0 to 100 are displayed using an identical false color scale. The dimensions of each image are approximately 24 × 32 mm. Scale bar, 10 mm.

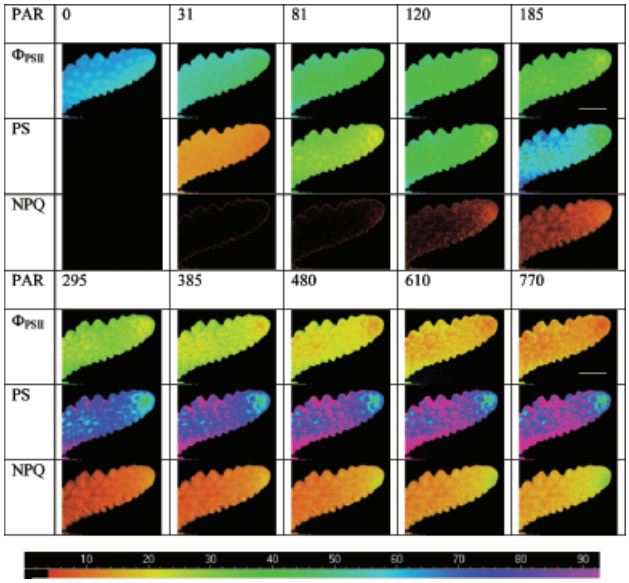

FIG. 3. Chl *a* fluorescence images of *Acropora nobilis* (sun-adapted branch) collected in the course of a rapid light curve recording with 10-s illumination steps. Data displayed are effective quantum yield (ΦPSII), relative photosynthesis rate (PS), and nonphotochemical quenching coefficient (NPQ). Relative values ranging from 0 to 100 are displayed using an identical false color scale. Dimensions of each image are approximately 24 × 32 mm. Scale bar, 10 mm.

absorptivity, the new photosynthetic parameter provided by the Imaging-PAM, showed distinct heterogeneity between polyp and coenosarc tissue for all three species, where *A. nobilis* and *P. decussata* had a lower absorptivity in the polyps (blue) and *G. australiensis* showed higher absorptivity in the polyps (purple) than in the coenosarc. A similar pattern was apparent in the F and F_m' images, both of which increased with increasing content of photosynthetically active pigments. Because Φ_{PSII} was calculated from a ratio of fluorescence parameters, the heterogeneities due to different pigment contents can be expected to disappear. Indeed, Φ_{PSII} was more similar for polyp and coenosarc than the fluorescence yields. The remaining heterogeneities reflected local differences in photosynthetic efficiency, with a tendency for a higher efficiency in the coenosarc regions of all three species.

The relative PS showed substantial heterogeneities for all three species. *Acropora nobilis* and *P. decussata* showed greater photosynthetic activity in the coenosarc tissues than in the polyp. In *A. nobilis* the tip of the branch showed distinctly lower activity than the basal region. *Goniastrea australiensis* had higher photosynthetic activity in the polyps than in the coenosarc due to the substantially higher absorptivity in this tissue region. Interestingly, there is even heterogeneity of photosynthetic activity within the polyps of *G. australiensis*. Although NPQ was rather low in all three species, it displayed pronounced heterogeneities. *Goniastrea australiensis* showed a higher NPQ inside the polyp, and *A. nobilis* had elevated levels of NPQ on the polyp walls and coenosarc.

Rapid light curves provided images of the various fluorescence parameters during exposure to increasing light levels. Although the chosen illumination time of 10 s was much too short for reaching a steady state, the observed responses reflected the current capacity of the corals to tolerate increases in light. The response of an *A. nobilis* branch to increasing irradiance is shown in Figure 3. Values of Φ_{PSII} decreased from 0.6 to less than 0.2 over the range of irradiance up to 770 µmol photons $\cdot m^{-2} \cdot s^{-1}$ and at the same time NPQ increased substantially (Fig. 4D). The relative PS increased following a typical saturation curve (Fig. 4C). In the course of this RLC characteristic heterogeneities developed. At 185 µmol photons $\cdot m^{-2} \cdot s^{-1}$, the tip of the *A. nobilis* branch showed a lower Φ_{PSII} relative to the rest of the branch. This differential response of the tip was also clearly evident in the PS series of images. Also, the NPQ response for the tip was clearly higher than that of the rest of the branch.

Figure 4 provides an indication of the variability of the RLC data (Fig. 3). The Imaging-PAM allows a large number of areas of interest to be defined. Here four

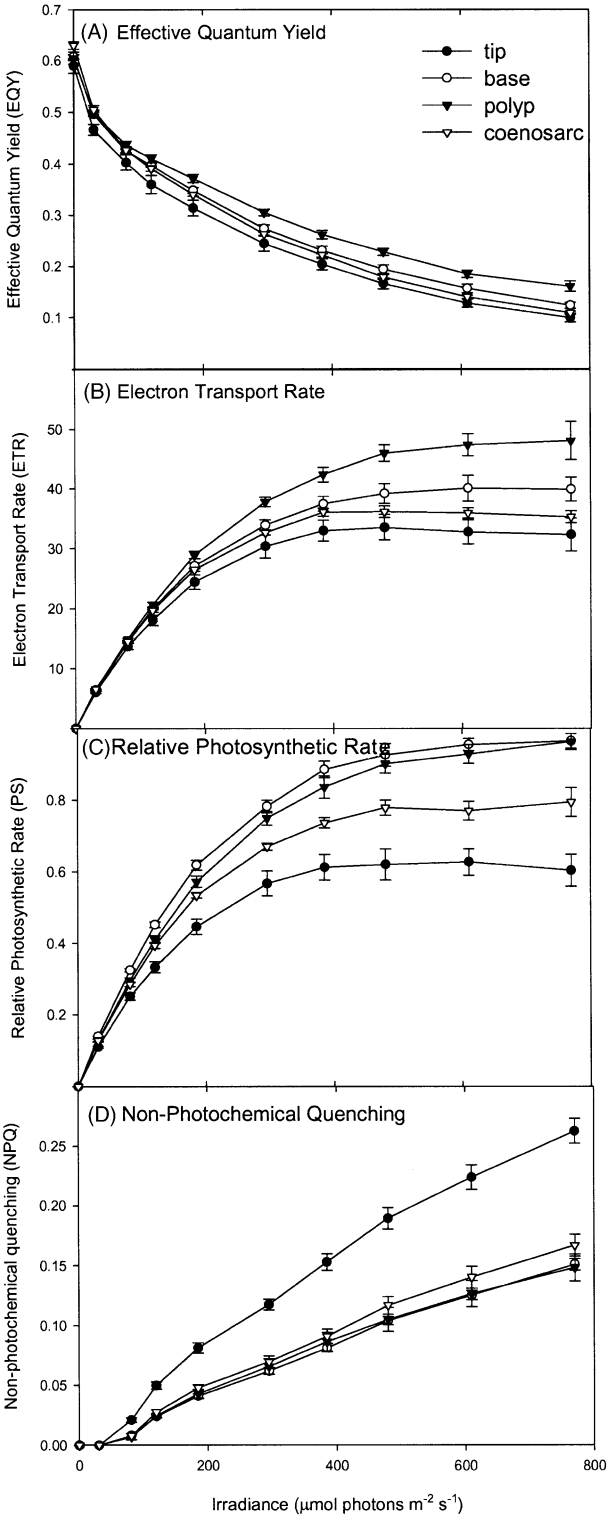

FIG. 4. Rapid light curve recordings of *Acropora nobilis* derived from the original images displayed in Figure 3. Areas of interest (AOIs) were defined in the polyp and coenosarc tissues and in the tip and basal regions. (A) Effective quantum yield, (B) ETR, (C) relative photosynthetic rate (PS), and (D) NPQ. Mean values with standard error of mean ($n = 4$).

sets of representative areas were chosen at the tip, base, polyp, and coenosarc regions. Within each area of interest, the pixel values were automatically averaged. The various area of interest data were plotted in the usual format of an RLC (Ralph et al. 2002). The ETR was fitted to a double exponential decay function (Eq. 1) and characteristic features of the RLC were derived (Table 1). Interestingly, the polyp showed the highest Φ_{PSII}, ETR, and PS (Fig. 4, A–C, respectively) with a significantly higher ETR_{max} (Table 1).

The tip of the *A. nobilis* branch showed a lower ETR than the basal region. Consistent with this observation, the E_k of the base and polyp samples was higher than that of the corresponding tip and coenosarc. The tip showed the largest NPQ response at all light levels.

Figure 5 shows the result of a photoinhibitory high-light treatment of *A. nobilis* and *P. decussa*ta. A 20-min exposure to 1000 µmol photons $\cdot m^{-2} \cdot s^{-1}$ caused dramatic changes in optimal PSII quantum yield (F_v/F_m), NPQ and PS responses, associated with development of definite spatial heterogeneity. Optimal PSII quantum yield (and PS) decreased in the regions exposed to high light, along with a corresponding increase in NPQ. The tip of the *A. nobilis* branch exposed to high light showed an increase in NPQ; correspondingly, the F_v/F_m and PS diminished. *Pavona decussata* did not appear to show the same degree of heterogeneity in response to high-light exposure, where the normally sun-exposed tissue (right-hand side of image) on the edge was similar to the more shade-adapted region (more distal, left-hand edge of the image).

Diel variations in incident irradiance caused changes in photosynthetic parameters (Fig. 6). Spatial heterogeneity was once again apparent, where polyps showed lower Φ_{PSII} around solar noon than coenosarc tissue in *A. nobilis*. To clearly illustrate the differences between polyp and coenosarc, three images had the color spectrum enhanced using the Imaging-PAM analysis function (Fig. 6B). This allowed relatively small heterogeneities to be emphasized. These enhanced images have been reprocessed by allocating the color spectrum to a smaller range of Φ_{PSII} from 0.3 to 0.6 (as seen on the color scale bar). Recovery from mid-day down-regulation and photoinhibition was almost complete by 8:00 p.m.

DISCUSSION

The application of high-resolution chl *a* fluorescence imaging has demonstrated that the complex topography of corals influences the photosynthetic activity of localized regions. Here we produced a quantitative map of chl *a* fluorescence yield of small sections of three corals and correlated this with structural topography (tip, base, polyp, and coenosarc). Previously, differences in the photosynthetic capacity of polyp and coenosarc tissue were shown from point measurements with fiberoptics using a Diving-PAM (1 mm) and Microfibre-PAM (140 µm) (Ralph et al. 2002). Here our RLC data show that polyps have a higher

TABLE 1. Curve fitting from RLC data from *Acropora nobilis* (Fig. 4B).

	Tip	Base	Polyp	Coenosarc	*P*
α	0.208 ± 0.009	0.221 ± 0.004	0.214 ± 0.003	0.224 ± 0.005	0.303
ETR_{max}	33.7 ± 2.19[a]	40.3 ± 2.03[a]	47.3 ± 1.66[b]	36.6 ± 0.91[a]	0.001*
E_k	162 ± 6.1[a]	182 ± 12.1[a]	220 ± 6.5[b]	164 ± 8.0[a]	0.001*

Values are means ± SE. One factor analysis of variance and Tukey's pairwise comparison for $P < 0.05$; superscript letters represent similar means; Asterisks represent significant difference $P < 0.05$.

ETR_{max} than coenosarc tissue. In the current study, variability of ETR_{max} within a colony was demonstrated, whereas the former study could discern variation only between colonies. Hill et al. (2004) used the same technology to examine the bleaching response; however, there was no difference between coenosarc and polyp of *A. nobilis* samples under such conditions. Nevertheless, our results suggest that most photosynthetic variability lies in the polyp/coenosarc tissue differentiation, but also with contributions from light and age gradients, such as along a branch. Although spatial heterogeneity in coral photosynthesis has been documented before (Falkowski et al. 1984, Gladfelter et al. 1989, Kühl et al. 1995), this is the first time it has been documented in such detail.

The light climate appears to influence the relative photosynthetic activity of the coenosarc and polyp tissues of *A. nobilis*. Shade-adapted samples (Fig. 2 and 6) showed the coenosarc tissue to have a greater Φ_{PSII} than polyps, corresponding to the pattern found with *A. nobilis* adapted to 50 μmol photons $\cdot m^{-2} \cdot s^{-1}$ in our previous investigation (Ralph et al. 2002). However, the sun-adapted specimens (Figs. 3–5) showed a higher Φ_{PSII} in the polyp tissue. Hill et al. (2004) used sun-adapted samples but was unable to differentiate the Φ_{PSII} of polyp and coenosarc tissue. Differences between polyp and coenosarc tissue will be influenced by the light climate of the zooxanthellae in each situation. Fitt and Cook (2001) found that the host tissue reduced the light reaching the zooxanthellae by at least 50%. Such a reduction would be increased within the polyp by self-shading from other zooxanthellae. Thus, zooxanthellae located deep within a polyp may be exposed to subsaturating irradiance at all times. In contrast, zooxanthellae within the coenosarc receive considerably more irradiance, and changes in Φ_{PSII} between the polyp and coenosarc tissues can be linked to coenosarc tissue suffering from greater photoinhibitory impact under elevated irradiance than the more protected polyp tissues.

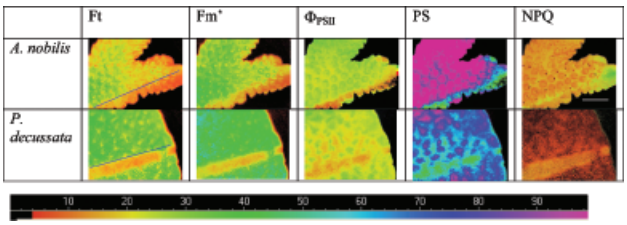

FIG. 5. Chl *a* fluorescence images of *Acropora nobilis* (sun-adapted) and Pavona decussata colonies after high-light exposure (20 min, 1000 μmol photons $\cdot m^{-2} s^{-1}$). Line in both Ft images indicates the upper edge of the high-light exposed region of the sample. Relative values ranging from 0 to 1 are displayed using an identical false color scale. Dimensions of each image are approximately 24 × 32 mm. Scale bar, 10 mm.

Although corals clearly have a complex surface topography, we imaged the most planar surfaces to avoid shadow effects. It is important, however, to realize that the illumination over the coral topography can vary significantly, and this will influence the measured chl *a* fluorescence signal. For example, this is apparent when comparing the images of the branch of *A. nobilis* to the moderately planar surface of *G. australiensis* (Fig. 2). Because of the curvature of the *A. nobilis* branch, the edges of the branch show lower F and F_m' signals as the curved sides of the branch received less measuring light (as well as less actinic light). In principle, topography effects are removed in all parameters based on ratios of fluorescence parameters, such as Φ_{PSII} and NPQ. But because the actinic irradiance is also lower in the curved areas, this influences the local values of Φ_{PSII} and NPQ. Nevertheless, we were able to demonstrate a systematic heterogeneity of Φ_{PSII} between polyp and coenosarc (Fig. 6B).

The tip of the *A. nobilis* branch was photoinhibited by high-light treatment, with a low ETR and elevated NPQ, but the effects were reversible once the tissue

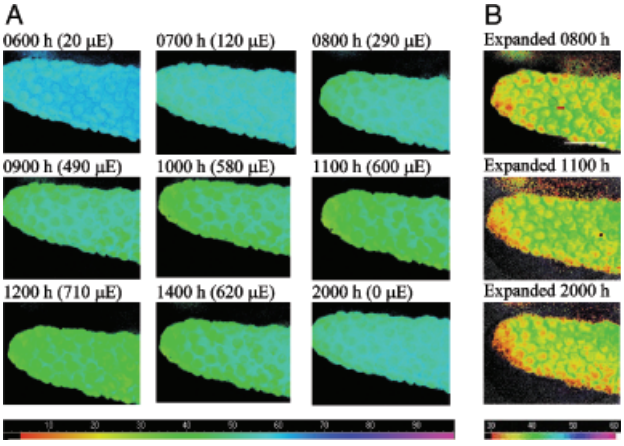

FIG. 6. Diel variation in ΦPSII of a shade-adapted *Acropora nobilis* branch. (A) PAR intensity (μE = μmol photons $\cdot m^{-2} \cdot s^{-1}$) is listed for each sample period. Relative values ranging from 0 to 100 are displayed using an identical false color scale. (B) Images (8:00 and 11:00 a.m. and 8:00 p.m.) were reprocessed to provide an expanded color scale (note different color bar below these images). Dimensions of each image are approximately 24 × 32 mm. Scale bar, 10 mm.

was returned to lower irradiance. The Φ_{PSII} showed a clear delineation with lower values around the tip of the branch. Tips of *Acropora* spp. have been found to have reduced zooxanthellar density (Gladfelter et al. 1989). Although our sample contained chl *a*, it was more vulnerable to light stress. Imaging of dynamic changes in chl *a* fluorescence allows insight into localized changes in photosynthetic function, such as fluctuations in light climate. Hill et al. (2004) thus illustrated a clear longitudinal gradient along *A. nobilis* branches exposed to bleaching conditions. We showed localized down-regulation of photosynthesis in the tip of *A. nobilis*, as did the diel samples that showed a lower Φ_{PSII} at the tip. The tip of the photoinhibited sample was considerably more damaged than the adjacent tissue slightly further down the branch (Fig. 5).

Fluorescence imaging can identify spatial patterns in chl distribution linked to epibiont organisms in corals (Simon-Blecher et al. 1996). In tissues where chl distribution is patchy (coenosarc and polyp) or correlated to topography, it is important to correct for variations in chl content when determining photosynthetic activity. This has significant implications for fluorescence-based estimation of photosynthetic ETR, because PAR absorption influences the rate of charge separation at PSII reaction centers. The Imaging-PAM offers a special routine, with which images of PAR absorption (absorptivity) are obtained. In this way, for the first time it has become possible to derive images of the estimated photosynthesis rate. By investigating spatial variation in photosynthetic parameters, it has become apparent that stress-induced responses are rarely continuous across the surface of a photosynthetic organism. The analysis of spatiotemporal variations with the Imaging-PAM can thus give important insights into the underlying mechanisms that control photosynthetic stress responses (Schreiber et al. 2003, Hill et al. 2004, Schreiber 2004).

The new chl *a* fluorescence imaging system used in this study allowed for a detailed spatiotemporal analysis of coral photosynthesis in relation to coral morphology and diel variations in irradiance. Diel variations in coral photosynthetic parameters have been described before (Ralph et al. 1999, Jones and Hoegh-Guldberg 2001, Lesser and Gorbanov 2001). We showed that the coenosarc of shade-adapted *A. nobilis* showed less down-regulation than adjacent polyp tissue under natural illumination. We speculate that a reduced Φ_{PSII} occurred under actinic light, which could have placed some pressure on the limiting steps of the photosynthetic apparatus, such that electrons accumulated at the acceptor side of PSII (Jones and Hoegh-Guldberg 2001). With increasing irradiance, the degree of PSII limitation increased. This pattern of heterogeneity was also seen in NPQ (Fig. 4C).

In conclusion, high-resolution fluorescence imaging allowed us to describe the complexity of coral photosynthetic parameters under various light conditions. Photosynthesis in corals exhibits distinct spatiotemporal heterogeneity, and chl fluorescence imaging is a convenient tool for early detection of spatially complex stress-induced damage (such as photoinhibition and diel down-regulation). We found a substantial variation in photosynthetic performance within a coral colony, along a branch, and between polyps and coenosarc. Thus, we could confirm the statement of Jokiel and Morrissey (1986) that it is unwise to extrapolate the physiological measurement of a single branch tip to the whole colony, because clearly numerous different habitats exist within a single colony.

Using chl imaging, the heterogeneity of photosynthesis in corals can now be studied at an unprecedented level of resolution. One of the most promising future applications of this new imaging system will allow the combination of high-resolution spatiotemporal photosynthesis measurements with fine scale sampling of coral tissue and analysis of zooxanthellae density and biodiversity.

We thank the staff of Heron Island Research Station for their support. Specimens were collected under Great Barrier Reef Marine Park Authority permit G01/623. The Australian Research Council, the University of Technology, Sydney, and the University of Sydney provided funding support for P. J. R. and A. W. D. L. M. K. was supported by the Danish National Science Research Council. C. W. Ralph is thanked for providing the coral illustration.

Berman-Frank, I., Lundgren, P., Chen, Y.-B., Küpper, H., Kolber, Z., Bergman, B. & Falkowski, P. 2001. Segregation of nitrogen fixation and oxygenic photosynthesis in the marine cyanobacterium *Trichodesmium*. *Science* 294:1534–7.

Björkman, O. & Demmig, B. 1987. Photon yield of O_2-evolution and chloroplast fluorescence characteristics at 77 K among vascular plants of diverse origins. *Planta* 170:489–504.

Chaerle, L. & van der Straeten, D. 2001. Seeing is believing: imaging techniques to monitor plant health. *Biochim. Biophys. Acta* 1519:153–66.

Daley, P. F., Raschke, K., Ball, J. T. & Berry, J. A. 1989. Topography of photosynthetic activity of leaves obtained from video images of chlorophyll fluorescence. *Plant Physiol.* 90:1233–8.

de Beer, D., Kühl, M., Stambler, N. & Vaki, L. 2000. A microsensor study of light enhanced Ca^{2+} uptake and photosynthesis in the reef-building hermatypic coral *Favia* sp. *Mar. Ecol. Prog. Ser.* 194:75–85.

Falkowski, P. G., Dubinsky, Z., Muscatine, L. & Porter, J. W. 1984. Light and the bioenergetics of a symbiotic coral. *Bioscience* 34:705–9.

Fitt, W. K. & Cook, C. 2001. The effects of feeding and addition of dissolved organic nutrients in maintaining the symbiosis between dinoflagellates and a tropical cnidarian. *Mar. Biol.* 139:507–17.

Gladfelter, E. H., Michel, G. & Sanfelici, A. 1989. Metabolic gradients along a branch of the reef coral *Acropora palmata*. *Bull. Mar. Sci.* 44:1166–73.

Grunwald, B. & Kühl, M. 2004. A system for imaging variable chlorophyll fluorescence in aquatic phototrophs. *Ophelia* 58:79–89.

Helmuth, B. S. T., Timmerman, B. E. H. & Sebens, K. P. 1997. Interplay of host morphology and symbiont microhabitat in coral aggregations. *Mar. Biol.* 130:1–10.

Hill, R., Schreiber, U., Gademann, R., Larkum, A. W. D., Kühl, M. & Ralph, P. J. 2004. Spatial heterogeneity of photosynthesis and the effect of temperature-induced bleaching conditions in three species of corals. *Mar. Biol.* 302:63–83.

Holub, O., Seufferheld, M. J., Gohlke, C., Govindjee & Clegg, R. M. 2000. Fluorescence lifetime imaging (FLI) in real time—a

new technique in photosynthetic research. *Photosynthetica* 38:581–99.

Jokiel, P. L., Lesser, M. P. & Ondrusek, M. E. 1997. UV-absorbing compounds in the coral *Pocillopora damicornis*: interactive effects of UV radiation, photosynthetically active radiation and flow. *Limnol. Oceanogr.* 42:1468–73.

Jokiel, P. L. & Morrissey, J. I. 1986. Influence of size on primary production in the reef coral *Pocillopora damicornis* and the macroalga *Acanthophora spicifera*. *Mar. Biol.* 91:15–26.

Jones, R. J. & Hoegh-Guldberg, O. 2001. Diurnal changes in the photochemical efficiency of the symbiotic dinoflagellates (Dinophyceae) of corals: photoprotection, photoinactivation and the relationship to coral bleaching. *Plant Cell Environ.* 24:89–99.

Kühl, M., Cohen, Y., Dalsgaard, T., Barker, Jorgensen B. & Revsbech, N. P. 1995. Microenvironment and photosynthesis of zooxanthellae in scleractinian corals studies with microsensors for O_2, pH and light. *Mar. Ecol. Prog. Ser.* 117:159–72.

Lesser, M. P. & Gorbanov, M. Y. 2001. Diurnal and bathymetric changes in chlorophyll fluorescence yields of reef corals measured in situ with a fast repetition rate fluorometer. *Mar. Ecol. Prog. Ser.* 212:69–77.

Nedbal, L., Soukupova, J., Kaftan, D., Whitmarsh, J. & Trilek, M. 2000. Kinetic imaging of chlorophyll fluorescence using modulated light. *Photosynth. Res.* 66:3–12.

Omasa, K., Shimazaki, K. I., Aiga, I., Larcher, W. & Onoe, M. 1987. Image analysis of chlorophyll fluorescence transients for diagnosing the photosynthetic system of attached leaves. *Plant Physiol.* 84:748–52.

Oxborough, K. & Baker, N. R. 1997. An instrument capable of imaging chlorophyll *a* fluorescence from intact leaves at very low irradiance and at cellular and sub cellular levels of organization. *Plant Cell Environ.* 20:1473–83.

Oxborough, K., Hanlon, A. R. M., Underwood, G. J. C. & Baker, N. R. 2000. *In vivo* estimation of the photosystem II photochemical efficiency of individual microphytobenthos cells using high-resolution imaging of chlorophyll a fluorescence. *Limnol. Oceanogr.* 45:1420–5.

Platt, T., Gallegos, C. L. & Harrison, W. G. 1980. Photoinhibition of photosynthesis in natural assemblages of marine phytoplankton. *J. Mar. Res.* 38:687–701.

Ralph, P. J., Gademann, R., Larkum, A. W. D. & Kühl, M. 2002. Spatial heterogeneity in active chlorophyll fluorescence and PSII activity of coral tissues. *Mar. Biol.* 141:639–46.

Ralph, P. J., Larkum, A. W. D., Gademann, R. & Schreiber, U. 1999. Photosynthetic responses of coral reef endosymbionts. *Mar. Ecol. Prog. Ser.* 180:139–47.

Rowan, R. & Knowlton, N. 1995. Intraspecific diversity and ecological zonation in coral-algal symbiosis. *Proc. Natl. Acad. Sci. USA* 92:2850–3.

Schreiber, U. 2004. Pulse-amplitude (PAM) fluorometry and saturation pulse method. In Papageorgiou, G. & Govindjee [Eds.] *Chlorophyll Fluorescence: A Signature of Photosynthesis*. Advances in Photosynthesis and Respiration Series. Kluwer Academic Publishers, Dordrecht, The Netherlands, pp. 279–319.

Schreiber, U., Gademann, R., Ralph, P. J. & Larkum, A. W. D. 1997. Assessment of photosynthetic performance of *Prochloron* in *Lissoclinum patella* by *in situ* and *in hospite* chlorophyll fluorescence measurements. *Plant Cell Physiol.* 38:945–51.

Schreiber, U., Walz, H. & Kolbowski, J. 2003. Propagation of spatial variations of chlorophyll fluorescence parameters in dandelion leaves induced by laser spot heating. http://www.pam-news.de/ar/03-01/PAMNews03-01.html

Siebke, K. & Weis, E. 1995a. Imaging of chlorophyll *a* fluorescence in leaves: topography of photosynthetic oscillations in leaves of *Glechoma hederaca*. *Photosynth. Res.* 45:225–37.

Siebke, K. & Weis, E. 1995b. Assimilation images of leaves of *Glechoma hederaca*: analysis of non-synchronous stomata related oscillations. *Planta* 196:155–65.

Simon-Blecher, N., Achituv, Y. & Malik, Z. 1996. Effect of epibionts on the microdistribution of chlorophyll in corals and its detection by fluorescence spectral imaging. *Mar. Biol.* 126: 757–63.

Sokal, R. R. & Rohlf, F. J. 1995. *Biometry: the Principles and Practice of Statistics in Biological Research*. Freeman, New York, 887 pp.